



Cite this: DOI: 10.1039/c4cc08381d

Received 23rd October 2014,  
Accepted 2nd December 2014

DOI: 10.1039/c4cc08381d

www.rsc.org/chemcomm

# Oligo(ethylene glycol)-incorporated hybrid linear alkyl side chains for n-channel polymer semiconductors and their effect on the thin-film crystalline structure†

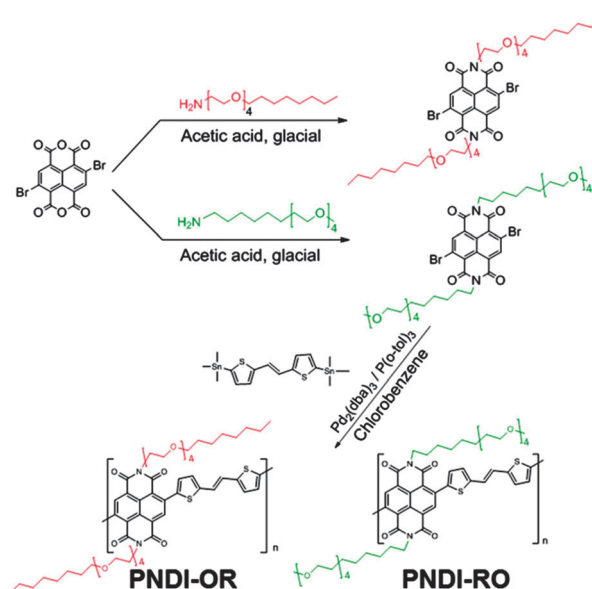
Ran Kim,<sup>‡a</sup> Boseok Kang,<sup>‡b</sup> Dong Hun Sin,<sup>b</sup> Hyun Ho Choi,<sup>b</sup> Soon-Ki Kwon,<sup>\*c</sup> Yun-Hi Kim<sup>\*c</sup> and Kilwon Cho<sup>\*b</sup>

**Oligo(ethylene glycol)-incorporated hybrid linear alkyl side chains, serving as solubilizing groups, are designed and introduced into naphthalene-diimide-based n-channel copolymers. The synthesized polymers exhibit unipolar n-type operation with an electron mobility of up to  $1.64 \text{ cm}^2 \text{ V}^{-1} \text{ s}^{-1}$ , which demonstrates the usefulness of the hybrid side chains in polymer electronics applications.**

$\pi$ -Conjugated polymer semiconductors have been the subject of intense research in the recent decades because of their potential applications in low-cost large-area field-effect transistors (FETs) and solar cells.<sup>1–7</sup> One of the most distinctive features of these polymer semiconductors, as compared to their inorganic counterparts, is their solution processability, which results from the attached flexible side chains.<sup>8,9</sup> The attachment of side chains to a  $\pi$ -conjugated backbone affords satisfactory solubility for polymer purification and device fabrication.<sup>10</sup> The selection of side chains involves striking a balance, because they affect molecular packing, thin-film morphology, and consequently material's performance in devices.<sup>11</sup> In stark contrast to the tremendous efforts made in designing new  $\pi$ -conjugated building blocks, studies to develop new solubilizing groups are rare. Branched or linear alkyl chains, such as 2-hexyldecyl, 2-octyldecyl, 2-decyl-tetradecyl, hexyl, octyl, or decyl groups, have typically been introduced as solubilizing groups.<sup>10</sup> Recently, oligo(ethylene glycol) and siloxane-terminated alkyl chains have been introduced in applications of organic electronics and

expressed positive outlooks;<sup>11,12</sup> however, only limited efforts have been made to develop new solubilizing groups.

In the present study, we designed two new hybrid linear side chains by alternating the combination of hydrophobic alkyl chains (–R–) and hydrophilic oligo(ethylene glycol) chains (–O–). Upon incorporating new side chains, electron-accepting naphthalene diimide (NDI) units and thienylene-vinylene-thienylene (TVT) units for extending the conjugation length were alternately coupled together (Scheme 1).<sup>13,14</sup> In the copolymers,  $\pi$ -conjugated backbones are adjacent to oligo(ethylene glycol) groups (PNDI-OR) or alkyl chains (PNDI-RO), corresponding to the attached side chains in the NDI units. Both copolymers, PNDI-OR and PNDI-RO, were air stable and exhibited good crystalline ordering with superior polymer-chain rigidity. Transistor devices with the synthesized polymers exhibited unipolar n-type operation. In particular, PNDI-RO exhibited an



Scheme 1 Synthetic routes of copolymers with hybrid linear side chains.

<sup>a</sup> Department of Chemistry and RINS, Gyeongsang National University, 501 Jinju Daero, Jinju, 660-701, Korea. E-mail: ykim@gnu.ac.kr

<sup>b</sup> Department of Chemical Engineering, Pohang University of Science and Technology (POSTECH) and Center for Advanced Soft Electronics (CASE), Pohang 790-784, Korea. E-mail: kwcho@postech.ac.kr; Fax: +82-54-279-8291

<sup>c</sup> School of Materials Science & Engineering and ERI, Gyeongsang National University, 501 Jinju Daero, Jinju, 660-701, Korea. E-mail: skwon@gnu.ac.kr

† Electronic supplementary information (ESI) available. See DOI: 10.1039/c4cc08381d

‡ R. Kim and B. Kang contributed equally to this work.

electron mobility of up to  $1.64 \text{ cm}^2 \text{ V}^{-1} \text{ s}^{-1}$ , higher than that of the devices with PNDI-OR ( $\sim 0.1 \text{ cm}^2 \text{ V}^{-1} \text{ s}^{-1}$ ). These results demonstrate the usefulness of hybrid side chains in polymer semiconductors.

The synthesis of the monomer and PNDI-OR/RO copolymers is shown in Scheme 1. First, amines were obtained by the Gabriel synthesis, followed by tosylation and nucleophilic substitution. The imidization of dibromonaphthalene dianhydride and 3,6,9,12-tetraoxaicosan-1-amine or dibromonaphthalene dianhydride and 2,5,8,11-tetraoxanonadecan-19-amine was performed in acetic acid. PNDI-OR and PNDI-RO were synthesized by the Stille coupling reaction. Detailed procedures are provided in the ESI.† The obtained polymers were purified by successive Soxhlet extraction with methanol, acetone, hexane, toluene, and chloroform. After Soxhlet extraction, the polymer was reprecipitated into methanol. The structure of the monomers and polymers was confirmed by  $^1\text{H-NMR}$  and IR (see the Synthesis section in the ESI†). Both PNDI-OR and PNDI-RO exhibited good solubility in common organic solvents such as chloroform and chlorobenzene because of the newly introduced side chains. The number average molecular weights ( $M_n$ ) of polymers were determined by gel permeation chromatography (GPC) analysis against polystyrene standards using chloroform as the solvent. PNDI-OR and PNDI-RO had  $M_n$  values of 16 500 and 24 300 with polydispersity indexes (PDIs) of 2.74 and 2.89, respectively.

The UV-vis absorption spectra of two copolymers are shown in Fig. 1a, and their optical, thermal, and electrochemical data are summarized in Table 1. The polymers exhibited typical dual-band absorption, where band I (530–900 nm) represents the typical intramolecular charge-transfer absorption resulting from the donor-acceptor structures of the polymers.<sup>15</sup> The optical band gaps ( $E_g$ , eV) of the polymers were calculated from the absorption edges; they were found to be 1.36 eV and 1.32 eV for PNDI-RO and PNDI-OR, respectively. The distinct shoulders

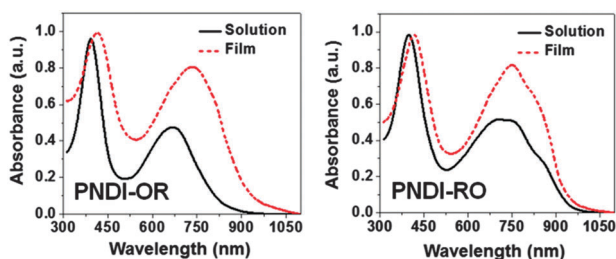


Fig. 1 Normalized absorption spectra in solution ( $\text{CHCl}_3$ ) and thin films of PNDI-OR and PNDI-RO polymers.

Table 1 Physical properties of polymers

Polymers	$M_n$ (kDa)/ PDI <sup>a</sup>	$\lambda_{\text{max}}^{\text{sol}}$ (nm)	$\lambda_{\text{max}}^{\text{film}}$ (nm)	$E_g^b$ (eV)	$E_{\text{HOMO}}^c$ (eV)	$E_{\text{LUMO}}^c$ (eV)	$T_d$ (°C)
PNDI-OR	17/2.74	670	734	1.36	-5.28	-4.05	397
PNDI-RO	24/2.89	707	735	1.32	-5.30	-4.01	382

<sup>a</sup> Determined by GPC using polystyrene standards in chloroform as the eluent. <sup>b</sup> Estimated from the onset of the UV-vis spectrum. <sup>c</sup> Onset potentials vs.  $\text{Fc}/\text{Fc}^+$  ( $E_{\text{HOMO}} = -4.8 \text{ eV}$ ) as external reference.

(780 nm and 850 nm at band I) in the spectrum of PNDI-RO solution imply stronger aggregation characteristics of PNDI-RO compared to PNDI-OR. Cyclic voltammetry (CV) measurements of the two copolymers in thin films were performed to evaluate their electronic energy levels (Fig. S1, ESI†). The highest occupied molecular orbital (HOMO) and lowest unoccupied molecular orbital (LUMO) levels of PNDI-RO ( $-5.30 \text{ eV}$  and  $-4.01 \text{ eV}$ , respectively) were almost identical to those of PNDI-OR ( $-5.28 \text{ eV}$  and  $-4.05 \text{ eV}$ , respectively) regardless of the attached side chains. The LUMO levels of the two polymers were close to  $-4.0 \text{ eV}$ , which is suitable for n-channel materials and indicate superior air stability of the polymers.<sup>13</sup> Density functional theory (DFT) calculations performed using the B3LYP functional and the 6-31G\* basis set showed that for PNDI-OR and PNDI-RO, the LUMOs are well delocalized along the monomers, and the difference between the two polymers is negligible (Fig. S2, ESI†). Both the copolymers exhibited good thermal stability, with 5% weight loss ( $T_d$ ) near  $400 \text{ }^\circ\text{C}$ , as determined by thermogravimetric analysis (TGA) under nitrogen (Table 1 and Fig. S3a, ESI†). The thermal transition properties of the polymers were investigated by differential scanning calorimetry (DSC); however, no distinct peak was observed (Fig. S3b, ESI†).

The thin-film morphologies of the two copolymers were investigated by atomic force microscopy (AFM) (insets of Fig. 2a). The morphologies of the as-spun thin films were quite different.

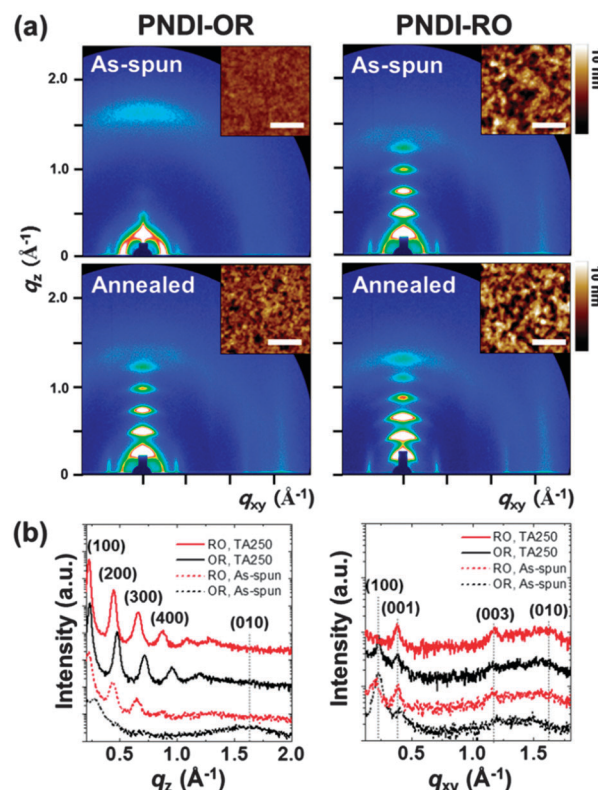


Fig. 2 (a) 2D GIXD patterns of PNDI-OR (left) and PNDI-RO (right) thin films as-spun and after thermal annealing at  $250 \text{ }^\circ\text{C}$ . The insets are AFM height images of the corresponding thin films, where the scale bars are  $200 \text{ nm}$ . (b) The corresponding GIXD diffractogram profiles along the out-of-plane and in-plane directions, where TA denotes thermally annealed.

The as-spun PNDI-OR thin films exhibited a smooth and flat surface, whereas the PNDI-RO thin films exhibited large interconnected grains. After annealing at 250 °C, both the copolymer thin films became rougher, and the size of the grains increased. It is noteworthy that PNDI-RO exhibited grains that were markedly larger (~120 nm in diameter) than those of PNDI-OR (~50 nm in diameter). Therefore, we believe that, compared with PNDI-OR, PNDI-RO can substantially strengthen intermolecular interactions to form more interconnected crystalline grains, which would allow superior charge-transport characteristics.<sup>16</sup>

The crystalline nature and molecular orientation were further studied by two-dimensional grazing-incidence X-ray diffraction (2D GIXD) analysis. Fig. 2a shows the 2D GIXD patterns of the as-spun (top) and thermally annealed (at 250 °C, bottom) polymer thin films on octadecyltrimethoxysilane (OTS)-treated SiO<sub>2</sub>/Si substrates. In the 2D GIXD pattern of the as-spun PNDI-OR thin film, both (100) and (010) reflections were competitively observed along the out-of-plane direction, which confirmed that the film texture is bimodal, *i.e.*, face- and edge-on crystallites coexist.<sup>17</sup> After thermal annealing at 250 °C, (*h*00) reflections became stronger along the out-of-direction, while the (010) reflections disappeared (Fig. 2a and b). This implies that the edge-on texture is thermodynamically favorable and that the face-on crystallites are kinetically produced during the spin-casting process, both of which are possibly attributed to the low surface energy of hydrophobic alkyl side chains.<sup>18</sup> In contrast to the dramatic texture change of PNDI-OR, apparent edge-on textures with different peak intensities were observed for both the as-spun and thermally annealed PNDI-RO thin films. Considering that branched-alkyl NDI-based analogs typically have a bimodal texture,<sup>13,14,19</sup> the predominant edge-on texture of PNDI-RO is a notable feature. The lamellar *d*-spacings of the annealed PNDI-OR and PNDI-RO were found to differ (2.63 nm and 2.81 nm, respectively), which can be attributed to the difference in the length of the attached side chains; in this study, the carbon atoms in the –RO chain are one in excess with respect to those of the –OR chains. Interestingly, the  $\pi$ -stacking distance of PNDI-RO (0.39 nm) was slightly shorter than that of PNDI-OR (0.40 nm), and PNDI-RO had a longer  $\pi$ -stacking correlation length (see the details in Table S1, ESI†). We speculate that the  $\pi$ -stacking of conjugated planes might be somewhat disrupted because of the presence of the bulky ethylene glycol groups near the polymer backbones.<sup>20</sup> Furthermore, both polymer thin films exhibited two reflection peaks ((001) and (003)) with a distance of 1.63 nm, which corresponds to about half of the repeating unit length of both copolymers. Judging from the above 2D GIXD results, it is apparent that the attachment of the hybrid side chains does not impede the crystalline ordering of polymers or reduce the rigidity of polymer main chains.<sup>2</sup>

The electrical performance of both copolymers was evaluated by fabricating bottom-gate/top-contact PFET devices. The polymer thin films were prepared on OTS-treated SiO<sub>2</sub>/Si substrates by spin-casting a chloroform solution (7 mg mL<sup>-1</sup>) of these films and then thermal annealing for 20 min in a N<sub>2</sub> atmosphere, followed by depositing the Au source and drain electrodes (channel length and width are 150 and 1500  $\mu$ m,

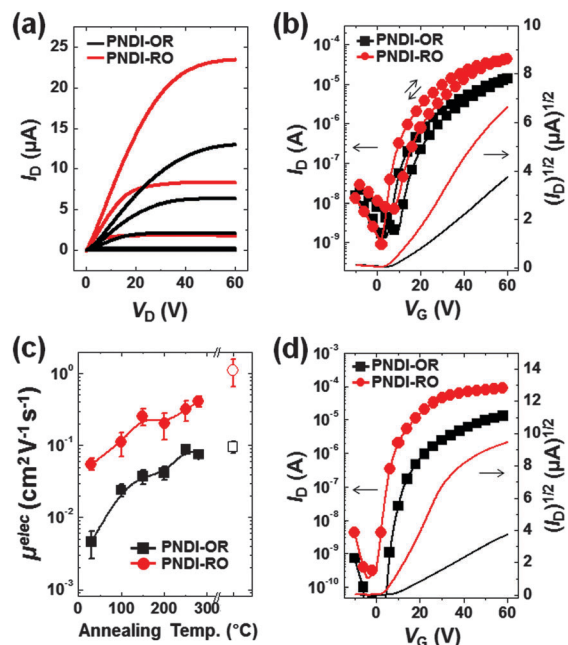


Fig. 3 Current–voltage characteristics of PFETs. (a) Output characteristics (gate voltage ( $V_G$ ) steps: 0, 15, 30, 45 and 60 V) and (b) transfer curves (drain voltage ( $V_D$ ) of 60 V) of PFETs based on PNDI-OR and PNDI-RO thin films after annealing at 250 °C. (c) Electron mobilities ( $\mu^{\text{elec}}$ ) as a function of annealing temperature, where open symbols indicate those of the devices fabricated using a 1-chloronaphthalene (CN) solvent additive. (d) Transfer curves ( $V_D = 60$  V) of the PFETs prepared using the CN additive.

respectively). Fig. 3a and b show the representative output and transfer characteristics of PFETs annealed at 250 °C. Both PNDI-OR and PNDI-RO exhibited unipolar n-channel field-effect behavior, mainly due to the low-lying HOMO levels;<sup>21,22</sup> hole mobility values were much lower than electron mobility values, ranging in the order of  $10^{-5}$  cm<sup>2</sup> V<sup>-1</sup> s<sup>-1</sup>. Thermal annealing resulted in significantly improved electron mobilities of both copolymers compared to the as-cast thin films (Fig. 3c and Table S2, ESI†). This result can be attributed to the improved crystalline ordering and enlarged crystalline domains after thermal annealing.

The annealed PNDI-RO films showed efficient n-channel operation with a high electron mobility of up to 0.51 cm<sup>2</sup> V<sup>-1</sup> s<sup>-1</sup> and a high on–off current ratio of  $10^6$ , as well as minor hysteresis during forward and backward sweeps. Moreover, the electrical characteristics of the annealed devices were almost unchanged after air exposure for three months. In contrast, about 5 times lower electron mobility ( $\sim 0.091$  cm<sup>2</sup> V<sup>-1</sup> s<sup>-1</sup>) was obtained for the annealed PNDI-OR. The charge-transport characteristics of PNDI-RO are superior to those of PNDI-OR, which can be attributed to the better long-range ordering of PNDI-RO, such as a shorter  $\pi$ -stacking distance with a longer correlation length (Table S1, ESI†) and morphologies of larger crystalline domains.<sup>1,3</sup> The performances of the devices based on the polymers are summarized in Table S2 in the ESI.†

In addition to the thermal annealing process, a solvent additive was introduced with the aim of further enhancing the performances of PFETs. 1-Chloronaphthalene (CN), which is

an organic solvent with a high boiling point of 259 °C,<sup>23</sup> was added to the polymer semiconductor–chloroform solution. The rest of the device fabrication was the same. The polymer films were annealed at the optimal thermal annealing temperature. Fig. 3d shows the transfer characteristics of PFETs prepared using 1.2 v% CN in chloroform. The CN-processed PNDI-RO FETs displayed a significantly enhanced electron mobility of up to 1.64 cm<sup>2</sup> V<sup>-1</sup> s<sup>-1</sup> (an average value of 1.12 cm<sup>2</sup> V<sup>-1</sup> s<sup>-1</sup>) with the bent transfer characteristics, which are very frequently observed in the literature about high-mobility polymer FETs.<sup>23</sup> PNDI-OR FETs also showed the enhanced mobility value of ~0.11 cm<sup>2</sup> V<sup>-1</sup> s<sup>-1</sup>, but the performance improvement is less pronounced compared to PNDI-RO. The root-mean-square (rms) roughness values of the thin films were increased after using the CN additive from 0.958 to 1.02 nm for PNDI-OR and from 1.77 to 3.71 nm for PNDI-RO (AFM images are provided in Fig. S3 in the ESI†). This is well correlated with the increase of field-effect mobility values. Therefore, the enhancement in the device performance can be attributed to the improved morphology and crystallinity, resulting from the reduced evaporation rate of the mixed solvent.

In addition, we tested the bias-stress stability of fabricated PFETs, where the PNDI-RO FETs exhibited more stable operation than did the PNDI-OR FETs. The better bias-stress stability of PNDI-RO FETs is presumably attributed to the aforementioned superior crystalline ordering and the difference in the chemical structure of the side chains (see Fig. S5, ESI†). Moreover, all-polymer bulk-heterojunction solar cells with all-polymer blend active layers consisting of PNDI-OR (or PNDI-RO) as an acceptor were tried as a further experiment. Interestingly, the blend film with PNDI-OR showed better power conversion efficiency, due to the appropriate degree of phase separation (see Fig. S6, ESI†).

In conclusion, oligo(ethylene glycol)-incorporated hybrid linear side chains were designed and synthesized with n-channel NDI-based copolymers (PNDI-OR and PNDI-RO). The microstructural ordering of the resulting polymers was altered according to the attached side chains, without disrupting the rigidity of the polymer main chain. Unipolar n-channel charge-transport behavior was observed for the resulting copolymers. In particular, PNDI-RO showed a high electron mobility of up to 1.64 cm<sup>2</sup> V<sup>-1</sup> s<sup>-1</sup> with a high on-off current ratio of 10<sup>5</sup>. These results demonstrate that hybrid side chains using oligo(ethylene glycol) are promising new solubilizing groups for high-performance organic semiconductor materials.

This work was supported by a grant (Code No. 2011-0031628 and 2013M3A6A5073172) from the Center for Advanced Soft

Electronics under the Global Frontier Research Program of the Ministry of Science, ICT and Future Planning, Korea. The authors thank the Pohang Accelerator Laboratory for providing the synchrotron radiation sources at 3C and 9A beam lines used in this study.

## Notes and references

- H. Sirringhaus, P. J. Brown, R. H. Friend, M. M. Nielsen, K. Bechgaard, B. M. W. Langeveld-Voss, A. J. H. Spiering, R. A. J. Janssen, E. W. Meijer, P. Herwig and D. M. de Leeuw, *Nature*, 1999, **401**, 685–688.
- I. McCulloch, M. Heeney, C. Bailey, K. Genevicius, I. Macdonald, M. Shkunov, D. Sparrowe, S. Tierney, R. Wagner, W. M. Zhang, M. L. Chabinyc, R. J. Kline, M. D. McGehee and M. F. Toney, *Nat. Mater.*, 2006, **5**, 328–333.
- R. J. Kline, M. D. McGehee and M. F. Toney, *Nat. Mater.*, 2006, **5**, 222–228.
- B. Kang, W. H. Lee and K. Cho, *ACS Appl. Mater. Interfaces*, 2013, **5**, 2302–2315.
- J. Soeda, H. Matsui, T. Okamoto, I. Osaka, K. Takimiya and J. Takeya, *Adv. Mater.*, 2014, **26**, 6430–6435.
- J. H. Cho, J. Lee, Y. Xia, B. Kim, Y. Y. He, M. J. Renn, T. P. Lodge and C. D. Frisbie, *Nat. Mater.*, 2008, **7**, 900–906.
- Y. D. Park, D. H. Kim, Y. Jang, M. Hwang, J. A. Lim and K. Cho, *Appl. Phys. Lett.*, 2005, **87**, 243509.
- T. Lei, J. Y. Wang and J. Pei, *Chem. Mater.*, 2014, **26**, 594–603.
- Y. J. Hwang, T. Earmme, S. Subramaniyan and S. A. Jenekhe, *Chem. Commun.*, 2014, **50**, 10801–10804.
- J. G. Mei and Z. N. Bao, *Chem. Mater.*, 2014, **26**, 604–615.
- J. G. Mei, D. H. Kim, A. L. Ayzner, M. F. Toney and Z. A. Bao, *J. Am. Chem. Soc.*, 2011, **133**, 20130–20133.
- C. Kanimozhi, N. Yaacobi-Gross, K. W. Chou, A. Amassian, T. D. Anthopoulos and S. Patil, *J. Am. Chem. Soc.*, 2012, **134**, 16532–16535.
- R. Kim, P. S. K. Amegadze, I. Kang, H. J. Yun, Y. Y. Noh, S. K. Kwon and Y. H. Kim, *Adv. Funct. Mater.*, 2013, **23**, 5719–5727.
- H. J. Chen, Y. L. Guo, Z. P. Mao, G. Yu, J. Y. Huang, Y. Zhao and Y. Q. Liu, *Chem. Mater.*, 2013, **25**, 4835.
- G. B. Zhang, P. Li, L. X. Tang, J. X. Ma, X. H. Wang, H. B. Lu, B. Kang, K. Cho and L. Z. Qiu, *Chem. Commun.*, 2014, **50**, 3180–3183.
- B. Kang, M. Jang, Y. Chung, H. Kim, S. K. Kwak, J. H. Oh and K. Cho, *Nat. Commun.*, 2014, **5**, 4752–4758.
- I. Osaka, M. Saito, T. Koganezawa and K. Takimiya, *Adv. Mater.*, 2014, **26**, 331–338.
- D. V. Anokhin, L. I. Leshanskaya, A. A. Piryazev, D. K. Susarova, N. N. Dremova, E. V. Shcheglov, D. A. Ivanov, V. F. Razumov and P. A. Troshin, *Chem. Commun.*, 2014, **50**, 7639–7641.
- J. Rivnay, R. Steyrleuthner, L. H. Jimison, A. Casadei, Z. H. Chen, M. F. Toney, A. Facchetti, D. Neher and A. Salleo, *Macromolecules*, 2011, **44**, 5246–5255.
- T. Lei, Y. Cao, X. Zhou, Y. Peng, J. Bian and J. Pei, *Chem. Mater.*, 2012, **24**, 1762–1770.
- H. Yan, Z. H. Chen, Y. Zheng, C. Newman, J. R. Quinn, F. Dotz, M. Kastler and A. Facchetti, *Nature*, 2009, **457**, 679–687.
- J. Zaumseil and H. Sirringhaus, *Chem. Rev.*, 2007, **107**, 1296–1323.
- T. K. An, I. Kang, H. J. Yun, H. Cha, J. Hwang, S. Park, J. Kim, Y. J. Kim, D. S. Chung, S. K. Kwon, Y. H. Kim and C. E. Park, *Adv. Mater.*, 2013, **25**, 7003–7009.